

MAGNETIC BEHAVIOR OF NICKEL FERRITE NANOPARTICLES PREPARED BY CO-PRECIPIATION ROUTE

*K. MAAZ, A. MASHIATULLAH, R.M. QURESHI¹, N.K. QAZI, S. KARIM², G. ALI² and T. JAVED

Directorate of Technology, PINSTECH, P.O. Nilore, Islamabad, Pakistan

¹Directorate of Co-ordination, PINSTECH, P.O. Nilore, Islamabad, Pakistan

²Physics Division, PINSTECH, P.O. Nilore, Islamabad, Pakistan

(Received September 16, 2008 and accepted in revised form December 16, 2008)

Magnetic nanoparticles of nickel ferrite (NiFe_2O_4) have been synthesized by co-precipitation route using stable ferric and nickel salts with sodium hydroxide as the precipitating agent and oleic acid as the surfactant. X-ray Diffraction (XRD) and Transmission Electron Microscope (TEM) analyses confirmed the formation of single phase nickel ferrite nanoparticles in the range 8-28 nm. The size of the particles was observed to be increasing linearly with increasing annealing temperature of the sample. Typical blocking effects were observed below ~ 225 K for all the prepared samples. The superparamagnetic blocking temperature was found to be continuously increasing with increasing particle sizes that has been attributed to the increased effective anisotropy of the nanoparticles. The saturation moment of all the samples was found much below the bulk value of nickel ferrite that has been attributed to the disordered surface spins of these nanoparticles.

PACS: 73.63 -b; 75.50Gg; 75.50Tt; 75.70Rf

Keywords: Magnetic properties, Ferrite nanoparticles, Surface anisotropy, Magnetic materials

1. Introduction

Metal-oxide nanoparticles are currently a subject of immense interest because of their unusual optical, electronic and magnetic properties, which often differ from their bulk counterparts. Many of these properties make them very promising candidates for a variety of applications [1-9]. The magnetic character of the nanoparticles used in medical, electronic and recording industries depends crucially on size, shape, purity and magnetic stability of these nanoparticles. These particles should be single domain, pure phase and having high coercivity and moderate magnetization. From the application point of view, the superparamagnetic blocking temperature of the nanoparticles used for recording devices should be well above the room temperature. In biomedical applications, these nanoparticles are used as drug carriers to the areas of the body where conventional drug delivery systems may not work. The most significant properties of magnetic nanoparticles namely, magnetic saturation, coercivity, magnetization and

loss, change drastically as the size of the particles move down into the nano-metric range [10-12]. Among different ferrites the nano-sized nickel ferrite possesses attractive properties for application as soft magnets and low loss materials at high frequencies [13].

Conventional techniques for preparation of nanoparticles and nanowires include sol-gel processing, evaporation condensation, microemulsion technique, combustion method, spray pyrolysis, hydrothermal process and template assisted electrochemical synthesis [14-20]. Generally, in most types of nano-particles prepared by these methods, control of size and size distribution is difficult [1]. In order to overcome these difficulties coprecipitation method has been used for synthesis of these nanoparticles. In this method, nanometer size reactors for the formation of homogeneous nanoparticles of nickel ferrite have been used. To protect the oxidation of these nanoparticles from the atmospheric oxygen and also to stop their agglomeration, the particles are usually coated with surfactant and then dispersed

* Corresponding author : maaz@pinstech.org.pk

in some medium like sodium dodecyl sulfate (NaDS) or oleic acid [21, 22]. The advantage of this method over the others is that the control of production of ferrite particles, its size and size distribution is relatively easy and there is no need of extra mechanical or microwave heat treatments. In the present work, nickel ferrite (NiFe_2O_4) were prepared by coprecipitation technique. They were heat treated (annealed) at different temperatures (from 600 to 1000°C). Various magnetic properties of nickel ferrites nanoparticles have been explored as a function of particle size and temperature. This is the first detailed study of superparamagnetic blocking effects and coercivity of NiFe_2O_4 as a function of particle size in the range (8-28 nm) that has not been reported so far.

2. Synthesis and Experimental Setup

3.0 molar solution of sodium hydroxide (as the precipitating agent) was slowly mixed with salt solutions of 0.4 molar ferric chloride ($\text{FeCl}_3 \cdot 6\text{H}_2\text{O}$) and 0.2 molar nickel chloride ($\text{NiCl}_2 \cdot 6\text{H}_2\text{O}$). The pH of the solution was constantly monitored by the addition NaOH. The reactants were constantly stirred using a magnetic stirrer until a pH level of >12 was achieved. A specified amount of oleic acid (2-3 drops for total reacting solution of 75 ml) was added to the solution as the surfactant and coating material as described above. The liquid precipitate was then brought to a reaction temperature of 80°C and stirred for 40 minutes. The product was cooled to room temperature and then washed twice with distilled water and ethanol to remove unwanted impurities and excess surfactant from the prepared sample. The sample was centrifuged for 15 minutes at 2000 rpm and then dried overnight at above 80°C. The acquired substance was then grinded into a fine powder and then annealed for 10 hours at 600°C. The final product obtained as confirmed by X-ray diffraction and EDX to be magnetic nanoparticles of nickel ferrite (NiFe_2O_4) with inverse spinel structure. The physical characterization was performed by X-ray diffractometer (Model: X'Pert Philips, Holland, with $\text{Cu-K}\alpha$ $\lambda = 0.154056$ nm) and High Resolution Transmission Electron Microscope (HRTEM, 300 keV) (Model: JEM-3010, JEOL). Debye Scherrer formula was used for size determination using the strongest peak in the XRD pattern. The average sizes of the particles annealed at 600, 700, 800, 900 and 1000°C for 10 hrs were found to be 8, 11, 18, 24 and 28 ± 3 nm. The magnetic characterization was done by Vibrating Sample Magnetometer (VSM, Model 7300 Lake Shore, USA) with an applied field of ± 10 kOe. The

dependence of the particle size on annealing temperature was also studied.

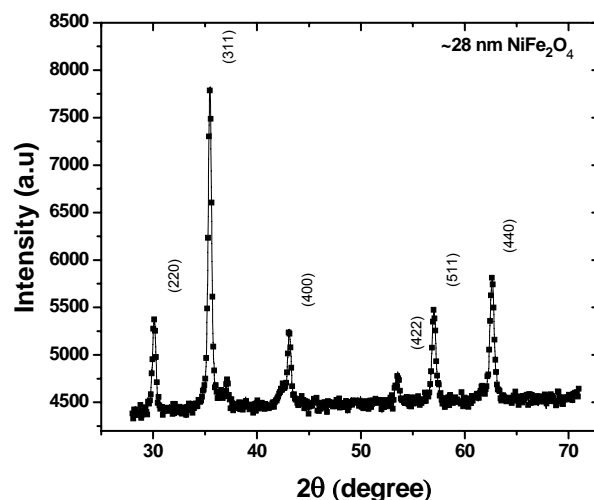


Figure 1. X-ray diffraction pattern of NiFe_2O_4 nanoparticles prepared by coprecipitation method, after annealing at 1000°C for 10 hrs with average crystallite size of about 28 nm.

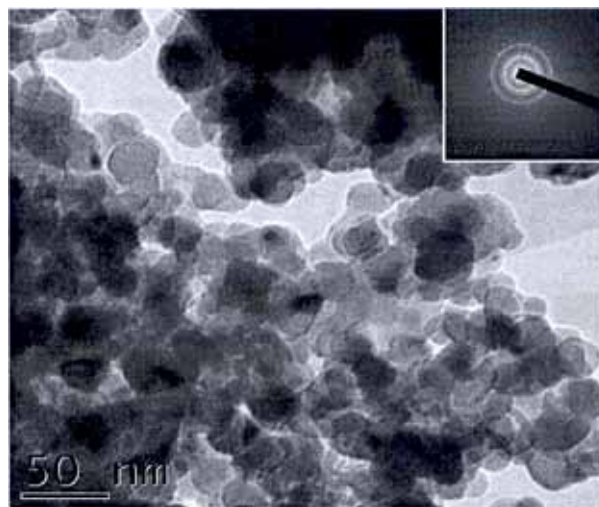


Figure 2. TEM micrograph of NiFe_2O_4 nanoparticles prepared, prepared by coprecipitation method, after annealing at 1000°C for 10 hrs.

3. Results and Discussion

The X-ray diffraction pattern (Fig.1) of the sample annealed at 1000°C prepared by coprecipitation technique shows that the final product is cubic spinel NiFe_2O_4 with average crystallite size of $\sim 28 \pm 3$ nm (the XRD peaks were compared to the standard PDF card number 742081 for inverse cubic nickel ferrite). Fig. 2 shows the high resolution TEM images of the same sample annealed at 1000°C for 10 hours (with average size of about 28 nm as determined by

XRD). In the TEM image most of the particles appear spherical in shape however some elongated particles are also present in the sample. The size variation in this study was varied from 8 to 28 nm with a distribution of ± 3 nm. Some moderately agglomerated particles as well as separated particles are present in the image. The inset of Fig. 2 shows the Selected Area Electron Diffraction (SAED) analysis of the sample indicating that the nanoparticles prepared are crystalline. The same has also been confirmed from the XRD peaks indicating the poly crystalline nature of the prepared sample. Fig. 3 shows the dependence of size of the particles on annealing temperature (T_{ann}). The size of the particles was observed to be increasing linearly with annealing temperature of the sample. It has been reported earlier that annealing process generally decreases the lattice defects and strains; however it can also cause coalescence of smaller grains that results in increasing the average grain size of the nanoparticles [23]. The observed increase in particle size with annealing temperature is most likely due to the fact that higher annealing temperature and time enhances the coalescence process resulting in an increase in the grain size. Thus it appears that particle size may be controlled by varying annealing temperature and time during the synthesis process.

Magnetic characterization of the particles was performed by vibrating sample magnetometer (VSM), between room temperature (300 K) and 77 K, with maximum applied field upto 10 kOe. Fig. 4 shows the $M(H)$ loops of 28 nm sample at room temperature (300 K) and 77 K. The insets of the figure show the expanded regions around the origin with different field ranges (± 400 and ± 1000 Oe) in order to make the coercivities at these temperatures visible. For the 28 nm size particles the coercivity at room temperature as depicted from the $M(H)$ loops was ~ 89 Oe while at 77 K it has increased to ~ 175 Oe. From Fig. 4 the saturation magnetization (M_s) obtained at room temperature was found to be ~ 40.5 emu/g, smaller than the bulk value of 56 emu/gm for nickel ferrite at room temperature, while at 77 K this value has increased to ~ 45 emu/g. The relatively large coercivity and saturation magnetization at 77 K are consistent with a pronounced growth of magnetic anisotropy inhibiting the alignment of the moment along applied field direction [24].

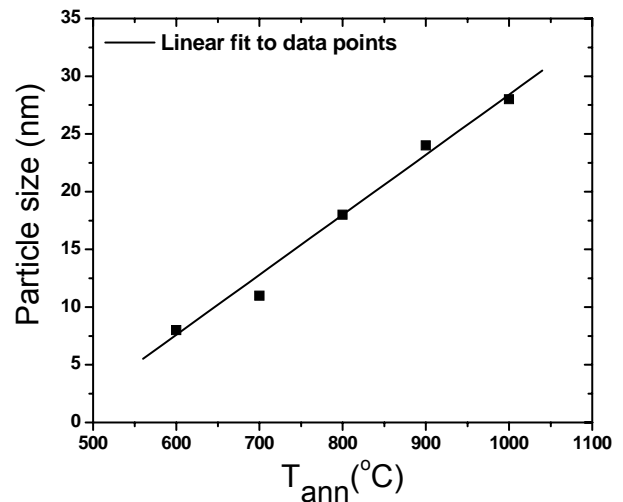


Figure 3. Particle size (nm) as a function of annealing temperature ($^{\circ}\text{C}$) for NiFe_2O_4 nanoparticles. annealed at 600, 700, 800, 900 and 1000°C with expected sizes of 8, 11, 18, 24 and 28 ± 3 nm respectively.

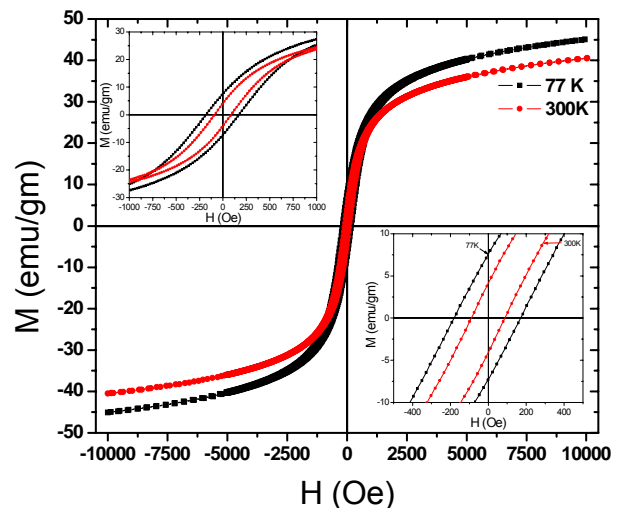


Figure 4. Hysteresis loops for 28 nm NiFe_2O_4 nanoparticles at room temperature (300 K) and 77 K at maximum applied field of 10 kOe.

The coactivity of the nanoparticles was also studied as a function of particle size at room temperature (300 K) as shown in Fig 5. The graph shows that for small sizes (8 to 11 nm), the coercivity increases with size rapidly, attaining a maximum value of ~ 175 Oe at ~ 11 nm and then decreases with size of the particles, for larger particles (12 to 28 nm). A ratio of the critical single domain radius for Ni-ferrite ($d_{\text{SD}}_{\text{Ni}}$) and Co-ferrite ($d_{\text{SD}}_{\text{Co}}$) has been calculated using the relation for critical single domain radius $d_{\text{SD}} = 36\kappa l_{\text{ex}}$; where κ is the magnetic hardness parameter defined by

$\kappa = (K_1 / \mu_0 M_S^2)^{1/2}$ [25]. For very hard magnetic materials $\kappa \gg 1$, while for very soft materials $\kappa \ll 1$. The exchange length (l_{ex}) is defined by $l_{ex} = (A / \mu_0 M_S^2)^{1/2}$ representing the length below which the atomic exchange interactions dominate the typical magnetostatic fields. For a typical permanent magnet the value of exchange length (l_{ex}) is of the order of 3 nm. The value of κ was calculated by taking the values of K_1 and M_S for bulk materials from Skomsky [25] while the value of l_{ex} was calculated by estimating the exchange constant (A) directly proportional to the respective T_C 's of Co- and Ni-ferrite. The ratio $[(d_{SD})_{Ni-ferrite}] / [(d_{SD})_{Co-ferrite}]$ was found to be ~ 0.38 . For a single domain limit of ~ 28 nm for $CoFe_2O_4$ as reported in one of our previous papers [26], this suggests d_{SD} for Ni-ferrite ~ 10.7 nm. We observed a maximum in $H_C - d$ curve (Fig. 5) for $NiFe_2O_4$ at ~ 11 nm. This value is much smaller than previously reported value of 14 nm for single domain limit of $NiFe_2O_4$ nanoparticles [12].

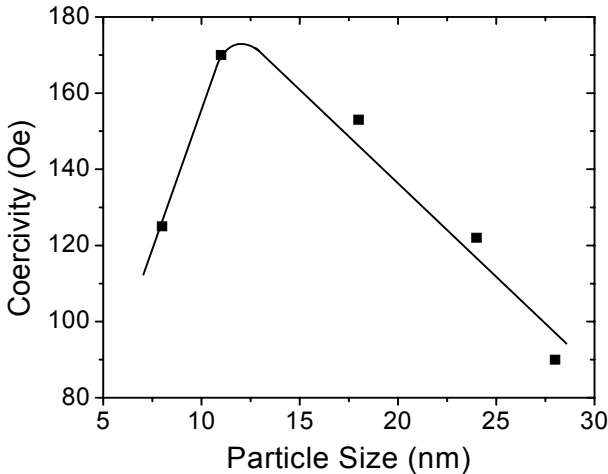


Figure 5. The coercivity (H_C) as a function of average particle diameter (nm) at room temperature. The peak of H_C at ~ 11 nm is evident in the data.

We noticed in Fig. 5 that the coercivity of nickel ferrite shows a non-monotonic behavior with particle size, i.e., for small sizes, the coercivity first increases, goes through peaks (at around 11 nm) and afterwards it decreases for larger particles, above the peak (12-28 nm). The initial increase of coercivity for smaller particles, below the peak, with increasing size may be assigned to the departure from the superparamagnetic state i.e., from unblocked to blocked state. This occurs for small particles when the thermal energy dominates the volume dependent anisotropy energy ($E_A =$

$K_{eff}V$). Hence, in the lower d region the coercivity may increase with increasing sizes, as the larger size particles would tend to show a blocked moment. The decline in H_C at higher value of d , above the peak, can occur due to the fact that as the particle size becomes large enough to sustain a domain wall. In this situation the magnetization reversal would occur via domain wall motion and consequently a lower coercivity would be observed. In $NiFe_2O_4$ however, this crossover is expected much higher than 11 nm where we observed the peak in our samples.

Fig. 6 shows the blocking temperature (T_b) depicted from the $M(T)$ curves of the samples as a function of particle size. The inset of the figure shows a typical zero field cooled (ZFC) $M(T)$ curve for one of the representative samples (with average size of 28 nm). For a single particle, at finite temperature, the ferromagnetically aligned magnetic moments fluctuate between their two energetically degenerate ground states on a time scale given by the relation [27]

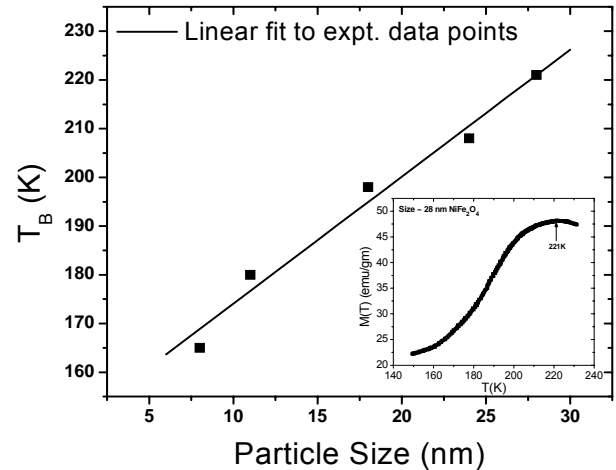


Figure 6. The dependence of superparamagnetic blocking temperature (T_B) on particle size (nm) for $NiFe_2O_4$ nanoparticles. The inset of the figure shows the temperature dependence of zero-field cooled (ZFC) magnetization.

$$\tau = \tau_0 \exp\left(\frac{K_{eff} V_p}{k_B T}\right)$$

where τ is the relaxation time and $K_{eff} V_p$ the effective anisotropy energy (E_A) of the particles. In Fig. 6 we see that there is a clear increase in the blocking temperature with size of the particles. The larger particles seem to be blocked at high temperatures as compared to the smaller particles. For larger particles, the larger volume causes increased anisotropy energy which decreases the

probability of a jump across the anisotropy barrier and hence the blocking is shifted to higher temperatures. Fig. 7 shows the dependence of saturation magnetization on particle size. The M_S values obtained for our samples varied between 9 to 40.5 emu/gm for the sizes 8 to 28 nm. The saturation magnetization increases consistently with size of the nanoparticles. The decrease in M_S at small sizes is attributed to the pronounced surface effects for smaller particles. The surface of the nanoparticles is considered to be composed of canted or disordered spins that prevent the core spins to align along the field direction, resultantly decreasing the saturation magnetization of the particles for smaller sizes of NiFe_2O_4 nanoparticles [28-30].

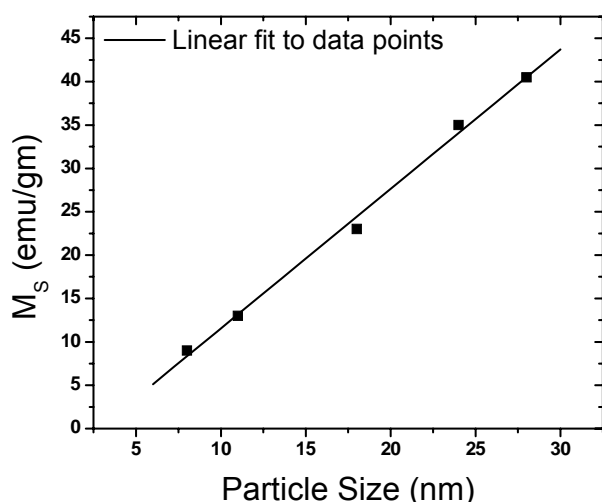


Figure. 7. Saturation magnetization (M_S) as function of particle size (nm) for NiFe_2O_4 nanoparticles. The observed values lie much below the bulk M_S value of ~ 56 emu/gm for NiFe_2O_4 .

4. Conclusions

In this article, we have presented synthesis of NiFe_2O_4 nanoparticles in the range 8-28 nm synthesized by coprecipitation route. The size of the particles was measured both by XRD and TEM and was found in good agreement with each other. The size of the particles appeared to increase linearly with annealing temperature most probably due to coalescence that increases with increasing temperature of annealing. The relatively large coercivity and saturation magnetization at 77 K in comparison with room temperature appeared to be due to the pronounced growth of magnetic anisotropy at low temperatures. The coercivity showed a peak with particle size at a value smaller than the previously reported value for single domain limit of NiFe_2O_4 and was attributed to the

enhanced role of the surface anisotropy as compared to the bulk for small sizes. The superparamagnetic blocking temperature was found to increase linearly with increasing particle sizes that was attributed to the increasing volume of the larger particles that resultantly increasing the effective anisotropy energy and hence the blocking temperature of nanoparticles. The smaller value of M_S for smaller particles was attributed to the disordered surface spins in nickel ferrite nanoparticles.

Acknowledgement

The author acknowledges PCSIR, Islamabad, Pakistan for providing six months abroad fellowship titled "Establishment of Nano-Tech Lab at PCSIR" and support from the Material Science Group-II, Institute of Modern Physics, Chinese Academy of Sciences, People's Republic of China for enabling this work.

References

- [1] M. Dariel, L.H. Bennett, D.S. Lashmore, P. Lubitz, M. Rubinstein, W.L. Lechter and M.Z. Harford, *J. Appl. Phys.* **61** (1987) 4067.
- [2] W.D. Williams and N. Giordano, *Phys. Rev. B* **33** (1986) 8146.
- [3] T.M. Whitney, J.S. Jiang, P.C. Searson and C.L. Chien, *Science* **261** (1993) 1316.
- [4] L. Piraux, J.M. George, J.F. Despres, C. Leroy, E. Ferain, R. Legras, K. Ounadjela and A. Fert, *Appl. Phys. Lett.* **65** (1994) 2484.
- [5] C.J. Brumlik and C. R. Martin, *Anal. Chem.* **59** (1992) 2625.
- [6] Z. Cai, C.R. Martin, *J. Amer. Chem. Soc.* **111** (1989) 4138.
- [7] S.K. Chakarvarti and J. Vetter, *Nucl. Instr. Meth. B* **62** (1991) 109.
- [8] Idem., *J. Microm. Microeng.* **3** (1993) 57.
- [9] Idem., *Radiat. Meas.* **29**, No. 2 (1998) 149.
- [10] I.M.L. Billas, A. Chatelain and W.A. de Heer, *Science* **265** (1994) 1682.
- [11] D.D. Awschalom and D.P.D. Vincenzo, *Physics Today* **48**, (1995) 43.
- [12] M. George, A.M. John, S.S. Nair, P.A. Joy and M.R. Anantharaman, *J. Magn. Mater.* **302** (2006) 190.
- [13] S. Son, M. Taheri, E. Carpenter, V.G. Harris and M.E. McHenry, *J. Appl. Phys.* **91**, No. 10 (2002) 7589.

- [14] D.H. Chen and Y.Y. Chen, *J. Colloid Interface Sci.* **9** (2001) 235.
- [15] J.J. Kingsley, K. Suresh and K.C. Patil, *J. Mater. Sci.* **25** (1990) 1305.
- [16] D.H. Chen and X.R. He, *Bull. Mater. Res.* **36**, (2001) 1369.
- [17] S.Z. Zhang and G.L. Messing, *J. Am. Ceram. Soc.* **73** (1990) 61.
- [18] D.H. Chen and Y.Y. Chen, *J. Colloid Interface Sci.* **41** (2001) 236.
- [19] J.L. Duan, J. Liu, H.J. Yao, Dan Mo, M.D. Hou, Y.M. Sun, Y.F. Chen and L. Zhang, *Materials Science and Engineering B* **147**, (2008) 57.
- [20] D. Mo, J. Liu, H.J. Yao, J.L. Duan, M.D. Hou, Y.M. Sun, Y.F. Chen, Z.H. Xue and L. Zhang, *J. Crystal Growth* **310** (2008) 612.
- [21] T. Feried, G. Shemer and G. Markovich, *Adv. Mater.* **13**, No.15 (2001) 1158.
- [22] C. Liu, A. J. Rondinone and Z. J. Zhang, *Pure Appl. Chem.* **72** Nos. 1-2, (2000) 37.
- [23] T. P. Raming, A. J. A. Winnubst, C. M. van Kats and P. Philipse, *J. Colloid and Interface Science* **249** (2002) 346.
- [24] A. Mumtaz, K. Maaz, B. Janjua, S.K. Hasanain and M.F. Bertino, *J. Magn. Magn. Mater.* **266** (2007) 313.
- [25] R. Skomski and J.D.M. Coey, "Permanent Magnetism", Institute of Physics Publishing Ltd., UK (1999).
- [26] K. Maaz, A. Mumtaz, S.K. Hasanain and A. Ceylan, *J. Magn. Magn. Mater.* **308** (2007) 289.
- [27] A. Aharoni, "Introduction to the theory of Ferromagnetism", Clarendon Press, Oxford 94 (1996).
- [28] A.E. Berkowitz, J.A. Lahut, I.S. Jacobs, L.M. Levinson and D.W. Forester, *Phys. Rev. Lett.* **34** (1975) 594.
- [29] A.E. Berkowitz, J.A. Lahut and C.E. Van Buren, *IEEE Trans. Magn.* **MAG-16** (1980) 184.
- [30] J.M.D. Coey, *Phys. Rev. Lett.* **27** (1971) 1140.